JOURNAL OF MATERIALS SCIENCE **39** (2004) 501–509

Interaction between cyclic loading and residual stresses in titanium matrix composites

J. M. HAUSMANN, C. LEYENS, W. A. KAYSSER
DLR—German Aerospace Center, Institute of Materials Research, Cologne, Germany (EU)
E-mail: joachim.hausmann@dlr.de

Metal matrix composites are gaining popularity for applications where high performance materials are needed. Titanium matrix composites (TMCs) continuously reinforced by silicon carbide fibres are under development for applications in aeroengines. Their use in blades, rings and shafts promises a significant weight reduction and performance improvement due to their high specific strength and stiffness. To obtain the whole capabilities of the material not only advanced processing techniques but also post-processing treatments are necessary. A detailed analysis of the residual stress development during cyclic loading leads to the necessity of residual stress modifications to optimise the fatigue behaviour of TMCs. Since the aerospace industry requires high reliability of the materials used, models for predicting failure and life time are of special interest. Predictive models based on the properties of the single constituents of the composite are most suitable to reduce the number of experiments and to develop methodologies to improve specific mechanical properties. Nevertheless, both experiments on the single constituents as well as on the composite are necessary to validate the model. A previously developed rheological model is used to assess different post-processing procedures to improve the fatigue behaviour of a titanium matrix composite. The usage of the model and experiments on the system SCS-6/Ti-6Al-2Sn-4Zr-2Mo are presented.

Symbols and indices

Symbols

A	Creep parameter
a, b	Creep exponents
B, C	Coffin-Manson parameter
E	Young's modulus
H	Hardening modulus
N	Cycles
n	Ramberg-Osgood exponent
R	Load ratio
T	Temperature
t	Time
v	Volume content
α	Coefficient of thermal expansion
ε	Strain
$\varepsilon'_{f,m}$, $\sigma'_{f,m}$	Coffin-Manson parameter
Δ	Difference
σ	Stress
σ'	Modified stress
σ_1	Elastic limit
σ_2	Maximum stress

Subscripts

a	Amplitude
b	Rupture
c	Composite
cr	Creep
el	Elastic
f	Fibre
IR	Irreversible fraction
m	Matrix
max	Maximum
pl	Plastic
Z	Residual strain resp. stress in fibre direction

1. Introduction

Relative to unreinforced titanium alloys, continuously silicon carbide fibre reinforced titanium matrix composites (Ti-MMCs or TMCs) offer higher strength and higher stiffness; furthermore, the reinforcement leads to a decrease of the density. Therefore, TMCs are among the most important candidate materials for high performance components in aeroengines such as compressor blades, vanes, shafts and rings [1–3]. All these components are highly fatigue loaded, thus the fatigue behaviour must be investigated and understood very well.

Due to the mismatch of the coefficients of thermal expansion (CTE) between fibre and matrix material, thermal residual stresses (TRS) are induced during cooling from processing to ambient temperature [4, 5]. The TRS leave the matrix in tension and thus support crack nucleation and propagation in this constituent. On the other hand the state of TRS may be altered by creep, yield and temperature effects. Consequently the fatigue

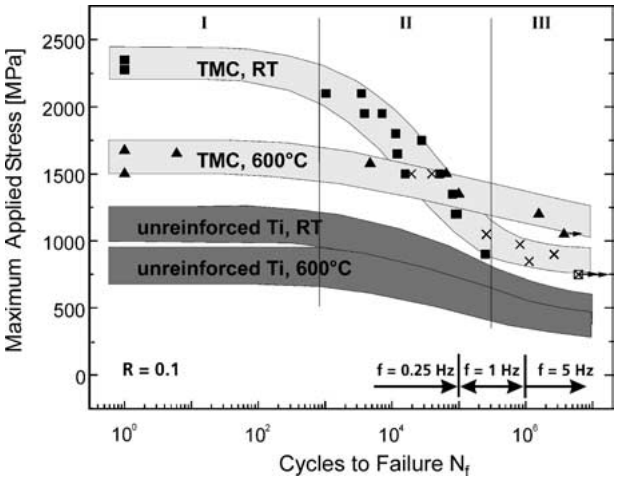

Figure 1 Wöhler-Curves of SCS-6/Timetal 834 and the unreinforced matrix alloy for $R = 0.1$.

failure mechanism of TMCs is closely related to the conditions and the load history the component is subjected to.

Fig. 1 shows the Wöhler curves for a TMC compared to the monolithic titanium alloy at room temperature and 600°C, respectively [6, 7]. The diagrams can be divided in three regions. Region I represents the low cycle fatigue (LCF) regime with a high stress level while region III is in the high cycle fatigue (HCF) regime with low stress levels and a transition zone (region II) in-between [8]. The classical fracture mechanics approach for metals relates HCF to loading below and LCF above yield limit [9]. This characterisation can certainly not be applied to TMCs since the fibres cannot deform plastic by itself and limit the total strain of the composite and, furthermore, the composite behaviour is strongly influenced by TRS [10–12].

To fully exploit the capabilities of TMCs, advanced processing techniques are needed. Inhomogenities and especially fibre-fibre contacts have to be avoided [10]. Therefore, the matrix coated fibre technique (MCF) has been established as most suitable since it leads to a fairly homogeneous fibre distribution without any binder, interweaving or other contamination [3]. Since the best coating quality can be achieved with the sputtering technique, all results presented in this paper are obtained from MCF fabricated TMCs using magnetron sputtering [4–6]. An overview of the complete processing route is given in Fig. 2.

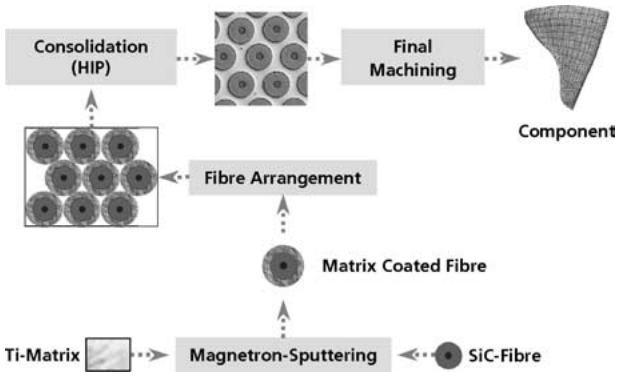

Figure 2 MCF-processing route for TMCs.

2. Loading-stress interaction

2.1. Influence of cyclic loading on residual stresses

Under LCF conditions at room temperature the matrix yields at the first cycle when the maximum stress is reached. Thus the state of the initial TRS is changed [13] by reducing the tensile stresses in the matrix and the compressive stresses in the fibres, respectively. This induces a load transfer from the matrix to the fibres. Consequently the fibres may fail in a cycle dependent manner although they are considered as fatigue resistant in this region. Due to the low rupture strain of the fibres and the ductility of the matrix a total failure of the composite cannot be induced by matrix failure. However, the fibres can fail successively until the load can no longer be sustained by the surrounding matrix. Curtin [14] and Assler [15] showed that clusters of at least 3–5 broken fibres are necessary to induce total failure of the composite. The small decrease of the Wöhler curve in this region is indicative of good fatigue resistance of the fibres.

Under HCF conditions at room temperature non gross plastic deformation of the matrix occurs. Due to TRS the matrix is in tension even in the unloaded TMC. Consequently, low applied stresses lead to a matrix stress which may be higher than the applied stress. In other words, the TMC is weakened by the reinforcement in this load case. The relatively low cyclic fatigue strength of the titanium alloy leads to matrix cracking. If the load is low enough to be carried by the fibres without causing failure, the matrix cracks are bridged by intact fibres [7]. Compared to LCF, the effectiveness of the reinforcement (strength of composite/strength of unreinforced matrix) under HCF conditions at room temperature is fairly low. Considering crack nucleation instead of total failure is even more critical for the composite.

Compared to room temperature TRS at 600°C are reduced by about 80%. Thus, for LCF conditions at 600°C, even at the first cycle, a higher fraction of stress is carried by the fibres. Since the fibre strength is less affected by temperature than the matrix strength, the beneficial effect of fibre reinforcement is higher compared to room temperature. At elevated temperatures the creep behaviour of the matrix alloy leads to a time and thus a frequency dependence. Similar to LCF at room temperature the maximum matrix stress is mainly independent of the applied stress; it is limited by the yield stress of the matrix.

At 600°C under HCF loading conditions the composite behaviour is strongly influenced by the creep behaviour of the matrix alloy. This means that under cyclic loading the matrix mean stress decays to zero at the applied cyclic mean stress of the composite. So the cyclic loads are carried mainly by the fibres. On the other hand, at cyclic minimum stress, the matrix can be in compression [16] even if tension-tension loading is applied. The very high fibre strength combined with an almost unloaded matrix leads to an excellent fatigue resistance of the TMC at high temperature.

Cyclic tension-compression loading ($R < 0$) differs from the tension-tension loading in two ways. First of all, irreversible deformations (creep and yielding) are

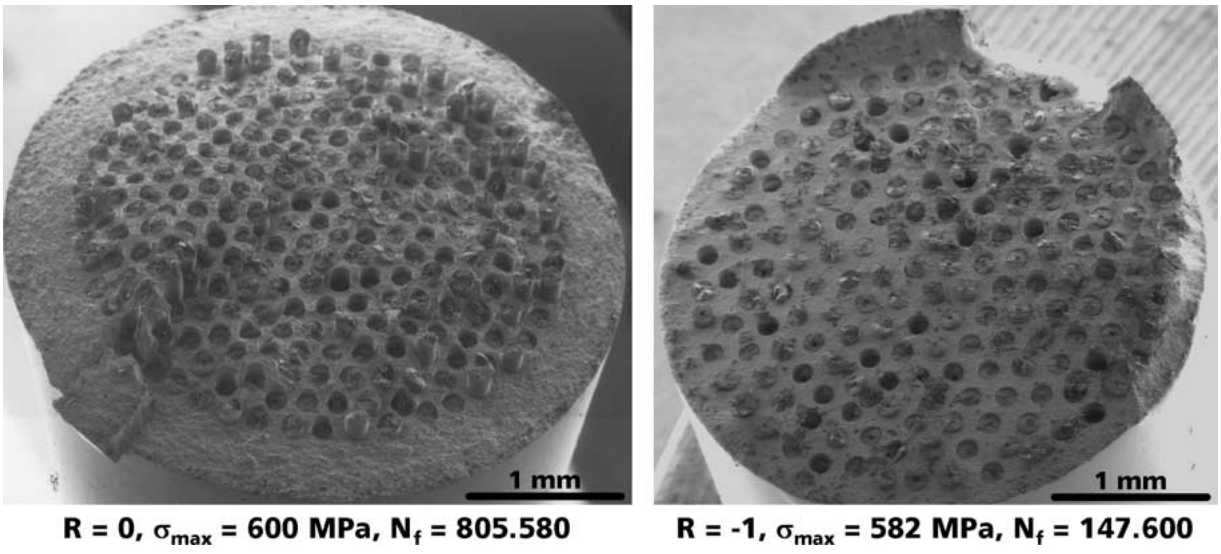

Figure 3 Comparison of the fracture surfaces under tension-tension loading (left) and tension-compression loading (right).

reduced. Thus the reduction of TRS is slower and the load distribution between fibres and matrix is more unfavourable. The second aspect concerns the behaviour in response to matrix cracks and thus especially the HCF behaviour at room temperature. Once the cracks are initiated, they open and close periodically. This leads to friction in the fibre-matrix interface [17] and shear stresses in the bridging fibres due to microscopic mismatch of the cracks while closing, resulting in a reduction of fibre strength and rapid failure of the composite. This leads to an even more pronounced loss in strength at room temperature under tension-compression HCF loading compared to the same conditions in the tension-tension mode [18]. Sometimes the HCF strength of the composite is even below that of the monolithic metal [19].

The phenomenon that matrix cracks initiate rapid fibre failure can be demonstrated by analyses of the fracture surfaces. Fig. 3 compares fracture surfaces of specimens tested under tension-tension and tension-compression loading, respectively. In the tension-tension mode the opened matrix crack induces shear failure of the fibre-matrix interface and thus fibre breakage occurs at the weakest location within the debonded length. A pronounced pull-out behaviour is the consequence. Under tension-compression loading the same debonding mechanisms occur. However, the fibres do not fail at their weakest point within the debonded length but are weakened by friction and shear forces in the region of the matrix cracks. The fracture surfaces of fibres and matrix are nearly in the same plane resulting in an apparent shorter debonded length. Even so it can be assumed that the debonding mechanism is similar in both cases, since the mechanisms of load sharing and fibre-matrix load transfer are depending on the materials properties and not on the loading conditions.

A further difference can be found in the ratio of the areas of fatigue crack and final fracture. In the tension-tension mode fatigue cracks in the matrix cover nearly the whole cross section before fracture. Final failure occurs mainly within the fibres. In contrast, in the tension-compression mode the fatigue crack in the matrix induces fibre failure and thus the final fracture occurs in both fibre and matrix leading to a larger fraction of the final failure surface. This is marked by a rough topography and significant shear lips.

2.2. Influence of residual stress modification on fatigue strength

The fatigue strength of TMCs is affected by residual stresses at room temperature and low stress levels only. This load case is marked by a very low effect of reinforcement. This phenomenon becomes more transparent by an analytical description carried out by the following steps:

1. For the example chosen the input properties are:

$$\Delta T = -680\ \text{K},\ \alpha_f = 4\ \text{ppm/K},\ \alpha_\text{m} = 11\ \text{ppm/K},$$
$$E_\text{f} = 400\ \text{GPa},\ E_\text{m} = 120\ \text{GPa},\ v_\text{f} = 40\%$$

2. Using

$$\sigma_{\text{m,z}} = \frac{\Delta T \cdot (\alpha_\text{f} - \alpha_\text{m})}{\frac{1}{E_\text{f}} \cdot \frac{1-v_\text{f}}{v_\text{f}} + \frac{1}{E_\text{m}}} \tag{1}$$

and

$$\sigma_{\text{f,z}} = -\frac{1 - v_\text{f}}{v_\text{f}} \cdot \sigma_{\text{m,z}} \tag{2}$$

the state of TRS can be obtained as: $\sigma_{\text{m,Z}} = 394$ MPa and $\sigma_{\text{f,z}} = -591$ MPa, respectively.

3. The corresponding strains are: $\varepsilon_{\text{m,z}} = 0,328\%$ and $\varepsilon_{\text{f,z}} = -0.148\%$, respectively.

4. For instance, if a stress amplitude of $\sigma_\text{a} = 550$ MPa is applied, which is of the order of the endurance limit of the unreinforced matrix material, under assumption of fully reversed loading $\sigma_\text{max} = -\sigma_\text{min} = \sigma_\text{a}$ the

maximum matrix stress is:

$$\sigma_{m,max} = E_m \cdot \left[\varepsilon_{m,z} + \frac{\sigma_a}{E_f \cdot v_f + E_m \cdot (1 - v_f)} \right] = 678 \text{ MPa} \quad (3)$$

On the other hand, the minimum matrix stress is:

$$\sigma_{m,min} = E_m \cdot \left[\varepsilon_{m,z} - \frac{\sigma_a}{E_f \cdot v_f + E_m \cdot (1 - v_f)} \right] = 109 \text{ MPa} \quad (4)$$

It is obvious, that the maximum matrix stress is significantly above the endurance limit of the matrix as well as the applied stress and thus the desired effect of reinforcement is missing. Although the load ratio R ($\sigma_{min}/\sigma_{max}$) is shifted to higher values by TRS the impact on life time improvement by load ratio correction is lower than the life time reduction by the higher maximum matrix stress.

5. The maximum stress in the fibres is:

$$\sigma_{f,max} = E_f \cdot \left[\varepsilon_{f,z} + \frac{\sigma_a}{E_f \cdot v_f + E_m \cdot (1 - v_f)} \right] = 356 \text{ MPa} \quad (5)$$

while the minimum stress is:

$$\sigma_{f,min} = E_f \cdot \left[\varepsilon_{f,z} - \frac{\sigma_a}{E_f \cdot v_f + E_m \cdot (1 - v_f)} \right] = -1540 \text{ MPa} \quad (6)$$

Thus the high strength fibres are loaded less than the matrix and their contribution of sustaining tensile loads is low. Otherwise, at minimum applied stress the fibres are loaded under high compression, thus shifting the R ratio of the fibres to lower values.

Under tension-tension loading matrix cracks may be bridged by intact fibres. A total failure is delayed or even avoided. Reversed loading leads to a more rapid fibre failure due to friction and shearing within the region of matrix cracks as discussed in the section before. Thus the maximum stress at crack initiation and the maximum stress at total failure are similar resulting in a substantial lower endurance limit under reversed loading compared to tension-tension loading.

Considering the influence of high tensile loads on the TRS state, it can be seen that a well defined pre-straining of the composite may reduce the TRS leading to improved HCF strength. This way of improving the fatigue strength of TMCs was proposed by [13] initially. Based on the analytical description given above, the influence of pre-straining can be analysed as follows:

6. Since a ductile matrix is required the composite can be strained up to the rupture strain of the weakest fibre reduced by the residual strain:

$$\varepsilon_{c,max} = \varepsilon_{f,b} - \varepsilon_{f,z} \quad (7)$$

Under the assumption of $\varepsilon_{f,b} = 0.75\%$ (the nominal rupture strain of SiC-fibres is 1%; under consideration of the natural scatter and a safety margin 0.75% is a conservative value) the allowed composite strain is $\varepsilon_{c,max} = 0.9\%$.

7. The fibres are ideal elastic and thus the fibre stress is:

$$\sigma_{f,0.9} = E_f \cdot \varepsilon_{v,max} - \sigma_{f,z} = E_f \cdot \varepsilon_{f,b} = 3000 \text{ MPa} \quad (8)$$

8. The matrix is considered as ideal elastoplastic with a yield stress of $\sigma_1 = 1000$ MPa. The elastic limit is exceeded resulting in a plastic strain $\varepsilon_{m,pl}$ of:

$$\varepsilon_{m,pl} = \varepsilon_{c,max} + \varepsilon_{m,z} - \frac{\sigma_1}{E_m} = 0.395\% \quad (9)$$

9. A fraction of the plastic matrix strain is transferred to the composite which obtains an irreversible strain $\varepsilon_{c,IR}$ of:

$$\varepsilon_{c,IR} = \frac{\varepsilon_{m,pl} \cdot E_m \cdot (1 - v_f)}{v_f \cdot E_f + (1 - v_f) \cdot E_m} = 0.122\% \quad (10)$$

10. The residual stresses after pre-straining are:

$$\sigma'_{m,z} = \sigma_{m,z} - \varepsilon_{m,pl} \cdot E_m + \varepsilon_{c,IR} \cdot E_m = 66 \text{ MPa} \quad (11)$$

and

$$\sigma'_{f,z} = \sigma_{f,z} + \varepsilon_{c,irr} \cdot E_f = -103 \text{ MPa} \quad (12)$$

A reduction of the residual stresses of about 83% compared to the "as processed" condition is obvious.

11. Repeating the loading of the composite in the same way as in the previous case with a stress amplitude of $\sigma_a = 550$ MPa leads to a maximum matrix stress of:

$$\sigma'_{m,max} = E_m \cdot \left[\varepsilon'_{m,z} + \frac{\sigma_a}{E_f \cdot v_f + E_m \cdot (1 - v_f)} \right] = 350 \text{ MPa} \quad (13)$$

The minimum matrix stress is:

$$\sigma'_{m,min} = E_m \cdot \left[\varepsilon'_{m,z} - \frac{\sigma_a}{E_f \cdot v_f + E_m \cdot (1 - v_f)} \right] = -219 \text{ MPa} \quad (14)$$

The maximum matrix stress is nearly 50% lower compared to the first case. Since this value is significant below the endurance limit of the matrix material, which is of the order of 550 MPa, an infinite life time can be expected at the given load.

12. The corresponding fibre stresses are:

$$\sigma'_{f,max} = E_f \cdot \left[\varepsilon'_{f,z} + \frac{\sigma_a}{E_f \cdot v_f + E_m \cdot (1 - v_f)} \right] = 845 \text{ MPa} \quad (15)$$

and

$$\sigma'_{f,min} = E_f \cdot \left[\varepsilon'_{f,z} - \frac{\sigma_a}{E_f \cdot v_f + E_m \cdot (1 - v_f)} \right] = -1051 \text{ MPa} \quad (16)$$

As desired and expected, now the fibres carry a higher load and the local load ratio of the constituents is closer to the applied load ratio.

If creeping of the matrix is included, the irreversible fraction needs to be added in step 8 to the plastic strain. A further reduction of residual stresses can be reached by this.

3. Model to analyse residual stress modification

To optimise post-processing treatments and to consider more complex mechanisms, as in the analysis above, a suitable model is needed. Finite element analysis would be possible but is too time and cost consuming for an optimisation cycle in parallel to the experiments. Furthermore, it is hard to distinguish the influence of different material parameters. Mathematical models are often very complex and difficult to apply to certain load cases. Rheological models consisting of spring, damper and slider may be the basis to develop models in a comprehensive and graphical way [9]. Each element of the model can be described by a physical law. The data for each element can be obtained from experiments addressing the special behaviour of the element. The suitable arrangement of the rheological elements to the complete model can be used to describe the combination of different mechanisms and even different materials, e.g., TMCs.

Fig. 4 shows the arrangement of elements to the rheological model for a continuous fibre reinforced metallic material under longitudinal loading. Fibre and matrix are connected in parallel such that they experience the same strain in fibre direction. Corresponding to the rule of mixture the stress is partitioned by the respective volume contents:

$$\sigma = v_\mathrm{f} \cdot \varepsilon \cdot E_\mathrm{f} + (1 - v_\mathrm{f}) \cdot (\varepsilon - \varepsilon_{\mathrm{pl,m}} - \varepsilon_{\mathrm{cr,m}}) \cdot E_\mathrm{m} \quad (17)$$

Due to its fully elastic behaviour the fibres are subjected to elastic strain only while the matrix strain contains irreversible portions.

In order to describe fracture of the constituents a fracture element is introduced. Below the fracture strength this element shows no response, thus it has an infinite stiffness. Exceeding the fracture strength leads to a stiffness of zero and any load is transferred to connected elements in parallel; if any exists. Otherwise total failure occurs. The fracture strength, especially that of the matrix, is a function of temperature and the loading mode, e.g., cyclic or static. Similar to the matrix strength, any element of the rheological model represents a mathematical function which is linear only in the most trivial case.

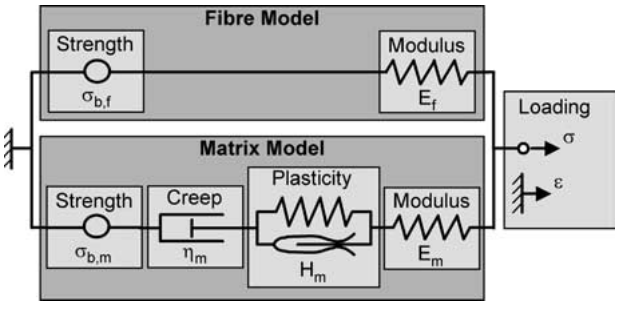

Figure 4 Modular set-up of the rheological model for continuous fibre reinforced MMCs under longitudinal loading.

3.1. Modules of the model

The fibre is described by its strength and modulus, both of which are mainly temperature dependent. In this approach plasticity, creep and cycle dependent behaviour is assumed irrelevant in the case of ceramic fibres. Furthermore, statistical aspects of the fibre properties are neglected; thus the mean property value is used in the computations.

The matrix behaviour is more complex. The strength is not only temperature dependent; it further depends on the number of applied load cycles and the load ratio. The strain-based approach for fatigue recommends the Coffin-Manson relationship [9, 20–22] to describe the cycle dependent strength under fully reversed loading:

$$\varepsilon_{\mathrm{a,m}} = \frac{\sigma'_{\mathrm{f,m}}}{E_\mathrm{m}} \cdot (2N)^\mathrm{B} + \varepsilon'_{\mathrm{f,m}} \cdot (2N)^\mathrm{C} \quad (18)$$

A suitable stress-strain relationship will be used to transfer the obtained strain into strength. Differences in the cyclic and static stress-strain response are neglected. The Smith-Watson-Topper-Equation [9] can be used to fit the results if load ratios other than $R = -1$ are present:

$$\sigma_{\max} = \frac{\sigma_{\mathrm{a,R=-1}}}{\sqrt{\frac{1-R}{2}}} \quad (19)$$

Since Equation 17 has shown an overestimation of the R-influence it shall be modified in such a manner that the correction influences just the difference between static and cyclic strength:

$$\sigma_{\max} = \sigma_2 - \sqrt{\frac{1-R}{2}} \cdot (\sigma_2 - \sigma_{\mathrm{a,R=-1}}) \quad (20)$$

A power law creep behaviour [9, 23] of the matrix may be considered:

$$\varepsilon_{\mathrm{cr,m}} = A \cdot \sigma_\mathrm{m}^\mathrm{a} \cdot t^\mathrm{b} \quad (21)$$

Some alloys used for TMCs as matrix material show significant creep rates not only at elevated temperatures but also at room temperature [24, 25]; its consideration depends on the loading conditions.

The plastic behaviour of the matrix material is strongly dependent on the metal alloy used and its microstructure. To describe this behaviour, different yield functions are suitable. Approaches such as the linear hardening may be used easily to describe the stress-strain behaviour:

$$\varepsilon(\sigma) = \begin{cases} \dfrac{\sigma}{E} \Big| 0 \le \sigma \le \sigma_1 \\ \dfrac{\sigma}{E} + \dfrac{\sigma}{H} \Big| \sigma > \sigma_1 \end{cases} \quad (22)$$

To prevent unrealistically high levels of stress under high strains it was decided to limit the stress by a maximum value σ_2. Matrix materials showing a soft transition from elastic to an ideal plastic yield regime may be described more accurately by the hyperbolic function [15, 26]:

$$\sigma(\varepsilon) = \begin{cases} E \cdot \varepsilon \Big| 0 \le \varepsilon \le \dfrac{\sigma_1}{E} \\ \sigma_1 + (\sigma_2 - \sigma_1) \cdot \tanh\left(\dfrac{E \cdot \varepsilon - \sigma_1}{\sigma_2 - \sigma_1}\right) \Big| \varepsilon > \dfrac{\sigma_1}{E} \end{cases} \tag{23}$$

The suitability of a yield function eventually depends on the matrix alloy and its microstructure. Independent of the yield function used, the plastic strain of the matrix is:

$$\varepsilon_{\mathrm{pl,m}} = \varepsilon - \frac{\sigma_{\mathrm{m}}}{E_{\mathrm{m}}} \tag{24}$$

Metallic alloys show the well known *Bauschinger Effect* [9, 27]. For instance, if a ductile material is deformed plastically under tension loading the elastic limit is shifted towards higher levels on further tension loading. Simultaneously the elastic limit under compression loading is reduced. This behaviour must be included in the model to analyse repeated loading correctly. The Young's modulus of the matrix is temperature dependent only. It can be described by any linear or power law.

Before using the model to evaluate the failure of TMCs some more aspects must be considered. These are thermal residual stresses, the load partitioning in the constituents and the influence of irreversible strains on the stress state.

3.2. Thermal residual stresses

TMCs are processed at higher temperatures than ambient temperature, and thermal residual stresses (TRS) are induced due to the mismatch of the coefficients of thermal expansion of the constituents. Equations to determine the stress components along the fibre axes, which are relevant in the case of longitudinal loading, have been used in Section 2.2 already (Equations 1 and 2). A fully elastic calculation can be performed if a reference temperature is considered at which the composite is assumed to be stress free [28, 29]. The stress state due to TRS is the starting condition for computation of the subsequent loading.

3.3. Stress partitioning in fibre and matrix

For failure analysis the partitioning of the applied stress in fibre and matrix is required to determine the weakest link in the composite. The balance condition requires:

$$\sigma = v_{\mathrm{f}} \cdot \sigma_{\mathrm{f}} + (1 - v_{\mathrm{f}}) \cdot \sigma_{\mathrm{m}} \tag{25}$$

To fulfil this condition thermal residual stresses and any strain fractions of the constituents must be considered. The assumption of fully elastic behaviour of the fibres enables determination of the fibre stress depending on the overall strain ε by:

$$\sigma_{\mathrm{f}} = E_{\mathrm{f}} \cdot \varepsilon + \sigma_{\mathrm{Z,f}} \tag{26}$$

The presence of plastic and creep strains of the matrix leads to:

$$\sigma_{\mathrm{m}} = E_{\mathrm{m}} \cdot (\varepsilon - \varepsilon_{\mathrm{pl,m}} - \varepsilon_{\mathrm{cr,m}}) + \sigma_{\mathrm{Z,m}} \tag{27}$$

Thus the stress partitioning not only depends on the Young's modulus of the constituents but also on the irreversible strains of the matrix.

3.4. Influence of irreversible matrix strains

If loading causes creep or plastic strains of the matrix, the state of residual stresses after unloading is altered. A fraction of the stress is transferred from the matrix onto the fibres. This is considered in the following analysis of loading since the stress partitioning depends on residual stresses as shown in Equations 26 and 27. The irreversible strain of the matrix is:

$$\varepsilon_{\mathrm{IR,m}} = \varepsilon_{\mathrm{pl,m}} + \varepsilon_{\mathrm{cr,m}} \tag{28}$$

The relations to re-compute the altered stress state are presented in Section 2.2 as Equations 9–12.

3.5. Determination of life time

This section describes the application of the model to evaluate the *Wöhler* curve of the TMC. A constant strain amplitude and frequency at a load ratio of $R = -1$ (tension-compression) is assumed. The constituent stresses for each load cycle can be determined iteratively as shown before. A comparison of the temperature- and cycle-dependent strength of the fibre and the matrix enables determination of failed constituents. Here, failure of one constituent is defined as total failure of the TMC.

Since thermal residual stresses are taken into account, the load ratio R of the constituents is not the same as the applied. In the special case of an applied load ratio of $R = -1$ the mean stress of the constituents is equal to the residual stress. Thus the maximum stress of the matrix is:

$$\sigma_{\mathrm{max,m}} = f(\sigma_{\mathrm{m}}(\varepsilon_{\mathrm{a}} + \varepsilon_{\mathrm{Z,m}})) \tag{29}$$

The stress-strain relationship $\sigma_{\mathrm{m}}(\varepsilon)$ (Equation 22 or 23) is used to consider the yield behaviour. Consequently the load ratio of the matrix is:

$$R = \frac{\varepsilon_{\mathrm{Z,m}} - \varepsilon_{\mathrm{a}}}{\varepsilon_{\mathrm{Z,m}} + \varepsilon_{\mathrm{a}}} \tag{30}$$

To consider the influence of the frequency a rectangular shaped cyclic loading is assumed. Thus the maximum loading is present in one half of the time while the minimum loading in the other half. This leads to a reduction

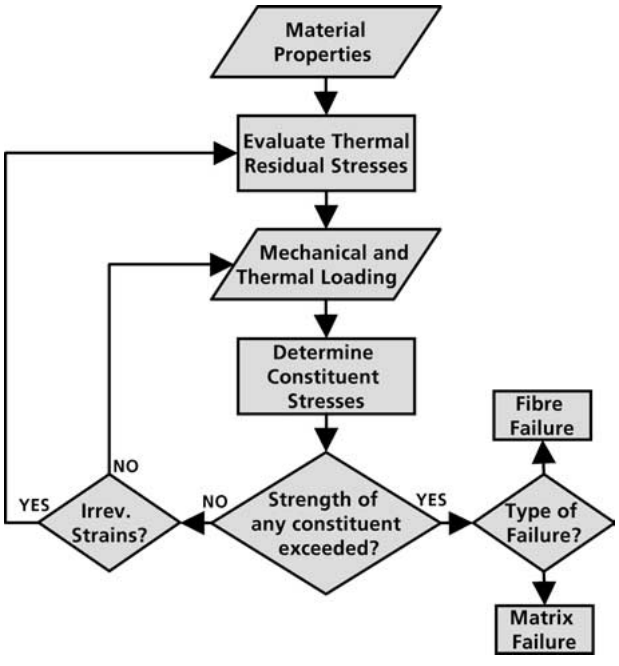

Figure 5 Algorithm to determine the *Wöhler* curve by the rheological model.

of the matrix stress due to creep of:

$$\Delta\sigma_{\max,m} = -E_m \cdot f\left(\varepsilon_{cr,m}\left(\sigma_{\max,m}, \frac{1}{2 \cdot f}\right)\right). \qquad (31)$$

In connection with

$$\varepsilon_{IR,m} = (\varepsilon_a + \varepsilon_{Z,m}) - \frac{f(\sigma_m(\varepsilon_a + \varepsilon_{Z,m}))}{E_m} + f\left(\varepsilon_{cr,m}\left(\sigma_{\max,m}, \frac{1}{2 \cdot f}\right)\right) \qquad (32)$$

and the procedure described in Section 2.2 the actual state of residual stresses can be determined. In the same way the stress state after loading under minimum load is determined. Starting with maximum load for the first cycle, which is the ultimate tensile strength (UTS) determined by the rule of mixtures, followed by a successive decrease enables the determination of the number of cycles to failure when the strength of one constituent is exceeded. This is cycle-dependent for the matrix and constant for the fibres. However, due to the load transfer by creep and yielding a cycle-dependent fibre failure may occur. Fig. 5 summarises the algorithm to determine the *Wöhler* curve.

4. Comparison of model and experiments

To demonstrate the usage of the model, it has been applied to a TMC which is a continuously silicon-carbide fibre reinforced near-α-titanium alloy, SCS-6/Ti-6Al-2Sn-4Zr-2Mo. The input properties are shown in Fig. 6. Following the procedure described above and via the algorithm shown in Fig. 5 the *Wöhler* curves of the composite are determined. Computation was done using a spreadsheet software. The result is shown in Fig. 7 along with some experiments data and the calculated strength

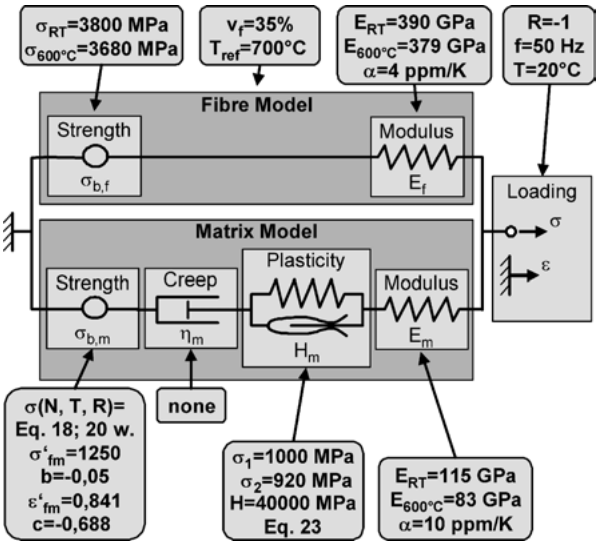

Figure 6 Input properties used in the analysis by the rheological model.

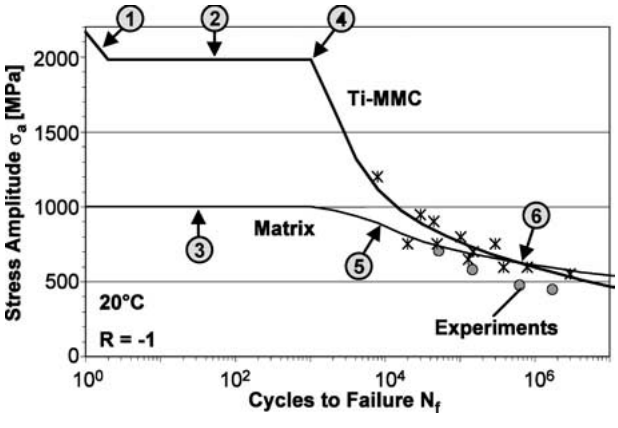

Figure 7 Wöhler curve of SCS-6/Ti-6Al-2Sn-4Zr-2Mo determined by the rheological model in comparison with experimental results obtained from SCS-6/Ti-6Al-2Sn-4Zr-2Mo (circles) [19] and SCS-6/Ti-6Al-4V (X) composites [31].

of the unreinforced matrix material by Equations 18 and 23 as reference. This curve contains distinct points which mark different effects. The first drop of the curve of the composite (1) is due to an elimination of thermal residual stresses during the first cycle by yielding. It happens only in this special load case which considers a constant strain amplitude and a constant mean stress of zero. Thus the mean strain increases corresponding to the irreversible strain $\varepsilon_{IR,c}$. After the second cycle the strength of the composite (2) as well as that of the unreinforced matrix (3) are nearly constant until approximately 1000 cycles. In this regime the strength of the composite is limited by the rupture strain of the fibres while the constant level of the strength of the matrix is due to the nearly ideal elastic-plastic behaviour of the titanium alloy; displaying the strain amplitude would show a significant decrease. In point (4) the curve for the composite shows a sudden drop which marks the transition from fibre- to matrix-induced failure. The strength of the matrix decreases simultaneously (5). At a very high number of cycles the strength of the composite drops even below that of the unreinforced material (6). This is caused by thermal residual stresses which are tensile in the matrix leading to premature

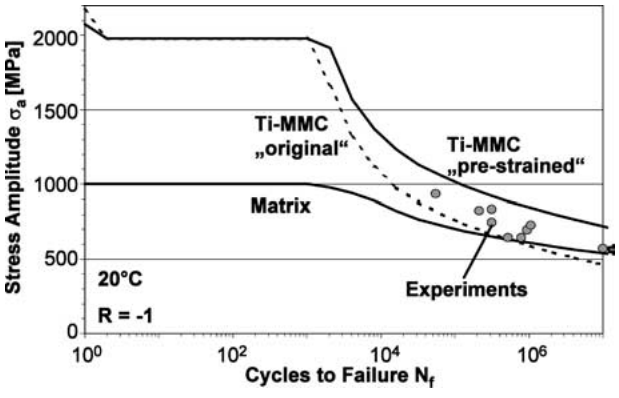

Figure 8 Effect of pre-straining as post-processing treatment on the fatigue behaviour of SCS-6/Ti-6Al-2Sn-4Zr-2Mo (results of model and experiments [19]).

crack initiation as described before. Such a behaviour was confirmed by experimental evidence. Experimental data is found in a region parallel to but somewhat below the predicted curve. The lower strength measured than predicted may be due to inhomogeneities in the material [10] as well as due to scatter of the properties of the constituents and the fibre volume content. Furthermore, the influence of multi-axial stresses induced by the three-dimensional nature of the residual stresses is neglected in the calculations. Thus the prediction reveals an upper limit for an ideal and defect free composite. Additionally, results of tests on SCS-6/Ti-6Al-4V are similar since the properties of Ti-6Al-4V are comparable with those of Ti-6Al-2Sn-4Zr-2Mo at room temperature.

In a second step the post-processing pre-straining procedure as described in Section 2.2 has been considered in the model as well as in the experiments. Fig. 8 shows the results. An improvement of about 30–40% of the HCF strength is obvious. Further improvement can be expected by optimisation of this treatment with the aid of creep effects. An influence on other fatigue regions (LCF and high temperature) by the TRS modification is not expected since this process induces irreversible deformations in a short time which would occur during the load history anyway. The UTS is reduced slightly due to reduced residual stresses by the pre-straining procedure while an improvement in the high cycle fatigue regime is obvious [30]. An elimination of the drop between the first and the second cycle would mark the total relaxation of residual stresses in fibre direction. Again the experimental results are somewhat below the prediction.

5. Discussion

Components loaded at high loads or at elevated temperatures can be reinforced by TMCs in an effective way. However, almost any component is running at low temperatures and low loads, too; at least during the starting process. In this case the composite is sensitive to matrix cracking if the TRS are not released before operation. The target is to develop a TMC which can be used in the entire temperature range from below room temperature up to 600°C. Post-processing treatments are suitable to modify the TRS in such a manner that the fatigue behaviour in the HCF regime at room temperature is improved drastically.

The presented model makes the optimisation process of the material easier and accelerates the development of suitable post-processing treatments. The lower strength measured than predicted may be due to inhomogeneities in the material as well as scatter of the properties of the constituents and the fibre volume content. Furthermore the influence of multi-axial stresses induced by the three-dimensional nature of the residual stresses is neglected. Thus the prediction reveals an upper limit for an ideal and defect free composite. Further reasons may be found in the microstructure of the matrix material which is totally different to unreinforced titanium alloys due to the influence of the magnetron sputtering process for the TMC processing. However, up to date there are no data for the sputtered titanium alloy which are suitable to create a matrix model. Nevertheless the tendency is obvious. Experiments to characterise the matrix material in a "composite-like" condition are planned to improve the input data.

6. Conclusions

The fatigue behaviour of TMCs differs significantly from that of monolithic metals. Therefore, a model to predict and optimise the fatigue behaviour has been developed which takes these differences into account. The following conclusions highlight distinct points of the model and its application.

- A suitable model for life time prediction of TMCs has to consider thermal residual stresses as well as the influence of irreversible matrix strains on residual stresses.
- A rheological model is developed which is suitable to predict the fatigue behaviour of TMCs under consideration of post-processing treatments.
- The modular set-up of the rheological model allows separate determination of specific properties of the constituents as input data and enables the detection of weak points of the composite.
- A modification of thermal residual stresses before HCF loading at room temperature improves the HCF strength substantially. Such a modification of thermal residual stresses can be reached by pre-straining of the composite.
- Under tension-tension loading matrix cracks may be bridged by intact fibres while fully reversed loading leads to rapid fibre failure inducing total failure. Thus the failure criterion assuming that failure of one constituent means composite failure is more accurate for fully reversed loading.

Acknowledgement

One of the authors (J. M. H.) would like to thank MTU AeroEngines for partial financial support of the research.

References

1. J. KUMPFERT, M. PETERS, U. SCHULZ and W. A. KAYSSER, in Proceedings of the European Conf. on Spacecraft Structures, Materials and Mechanical Testing, Braunschweig, 1999 (ESA, 1999) p. 315.
2. M. P. THOMAS, G. HOPWARD, R. PATHER, M. R. BROWN and P. TRANTER, *Int. J. Fatigue* **10** (2001) 851.
3. C. LEYENS, F. KOCIAN, J. HAUSMANN and W. A. KAYSSER, *Aerosp. Sci. Tech.* **7**(3) (2003) 201.
4. J. F. DURODOLA and B. DERBY, *Acta Met. Mater.* **5** (1994) 1525.
5. N. P. RANGSWAMY, M. B. PRIME, M. DAYMOND, M. A. M. BOURKE, B. CLAUSEN, H. CHON and N. P. JAYARAMAN, *Mater. Sci. Eng.* A **2** (1999) 209.
6. H. ASSLER, J. HEMPTENMACHER and K. H. TRAUTMANN, in Proceedings of the 4th International Conference on Low Cycle Fatigue and Elasto-Plastic Behaviour of Materials, Garmisch-Partenkirchen, Germany (1998) p. 461.
7. J. HEMPTENMACHER, P. W. M. PETERS, H. ASSLER and Z. XIA, in Proceedings of EUROMAT 99 (Munich, 2000) p. 190.
8. P. W. M. PETERS, Z. XIA, J. HEMPTENMACHER and H. ASSLER, *Composites* A **3/4** (2001) 561.
9. N. E. DOWLING, "Mechanical Behavior of Materials" (Prentice Hall, Upper Saddle River, 1999) p. 832.
10. J. HAUSMANN, J. HEMPTENMACHER and J. KUMPFERT, in Proceedings of the 13th International Conference on Composite Materials, edited by Y. Zhang (Beijing, China, June 2001), CD-R.
11. N. CHANDRA, C. R. ANANTH and H. GARMESTANI, *J. Comp. Tech. Res.* (1994) 37.
12. J. L. BOBET, C. MASUDA and Y. KAGAWA, *J. Mater. Sci.* **23** (1997) 6357.
13. D. S. LI and M. R. WISNOM, *J. Comp. Tech. Res.* **3** (1994) 225.
14. W. A. CURTIN and N. TAKEDA, *J. Comp. Mater.* **22** (1998) 2042.
15. H. ASSLER, "Charakterisierung und Modellierung der mechanischen Eigenschaften von SiC-faserverstärkten Titanmatrix-Verbundwerkstoffen," PhD-Thesis, RWTH Aachen, 1999, p. 170.
16. T. NICHOLAS, M. G. CASTELLI and M. L. GAMBONE, *Scr. Mater.* **5** (1997) 585.
17. T. E. STEYER, F. W. ZOK and P. D. WALLS, *Comp. Sci. Tech.* **10** (1998) 1583.
18. T. NICHOLAS, "Titanium Matrix Composites—Mechanical Behavior" (Technomic Publ. Co., Lancaster, 1998) p. 209.
19. J. HAUSMANN, C. LEYENS, J. HEMPTENMACHER and W. A. KAYSSER, in Proceedings of TMS Fall Meeting 2001 (Indianapolis, TMS Warendale, 2001) CD-R.
20. S. R. LAMPMAN, Fatigue and Fracture. "ASM Handbook. 19" (ASM International, Materials Park, OH, 1996) p. 1057.
21. D. MUNZ, "Ermüdungsverhalten metallischer Werkstoffe," (DGM, Oberursel, 1985) p. 484.
22. S. KOCANDA, "Series of Fatigue and Fracture" (Sijthoff & Noordhoff, Alphen, Netherlands, 1978) p. 379.
23. H. KRAUS, "Creep Analysis" (John Wiley & Sons, New York, 1980) p. 280.
24. T. NEERAJ, D.-H. HOU, G. S. DAEHN and M. J. MILLS, *Acta Mater.* **6** (2000) 1225.
25. H. J. FROST and M. F. ASHBY, "Deformation Mechanism Maps: The Plasticity and Creep of Metals and Ceramics" (Pergamon Press, Oxford, 1982) p. 166.
26. R. BOYER, G. WELSCH and E. W. COLLINGS, "Materials Properties Handbook: Titanium Alloys" (ASM International: Materials Park OH, 1994) p. 1169.
27. S. TIMOSKENKO, "Strength of Materials—Part II Advanced Theory and Problems" (Van Nostrand Reinhold Ltd., New York, 1958) p. 572.
28. S. G. WARRIER, P. RANGASWAMY, M. A. M. BOURKE and S. KRISHNAMURTHY, *Mater. Sci. Eng.* A **2** (1999) 220.
29. D. B. GUNDEL and D. B. MIRACLE, *Comp. Sci. Tech.* **10** (1998) 1571.
30. J. HAUSMANN, C. LEYENS, J. HEMPTENMACHER and W. A. KAYSSER, *Adv. Eng. Mater.* **7** (2002) 497.
31. H. J. DUDEK and R. LEUCHT, "Advanced Aerospace Materials" (Springer Verlag, Berlin, 1992) p. 124.

Received 29 January
and accepted 16 September 2003